forests

MDPI

Article

Thermal Modification and Alkyl Ketene Dimer Effects on the Surface Protection of Deodar Cedar (*Cedrus deodara* Roxb.) Wood

Teresa Lovaglio [1], Maurizio D'Auria [2], Wolfgang Gindl-Altmutter [3], Valentina Lo Giudice [1], Fausto Langerame [2], Anna Maria Salvi [2] and Luigi Todaro [1,*]

[1] School of Agricultural, Forestry, Food and Environmental Science, University of Basilicata, V.le Ateneo Lucano 10, 85100 Potenza, Italy
[2] Department of Science, University of Basilicata, V.le Ateneo Lucano 10, 85100 Potenza, Italy
[3] Department of Material Sciences and Process Engineering, Institute of Wood Technology and Renewable Materials, University of Natural Resources and Life Sciences Vienna, Konrad-Lorenz-Straße 24, 3430 Vienna, Austria
* Correspondence: luigi.todaro@unibas.it

Abstract: The aim of this research was to evaluate the multiple effects of both thermal modification and alkyl ketene dimer (AKD) on the deodar cedar (*Cedrus deodara* Roxb.) wood surface, before and after an irradiation test. The physical and chemical changes that occurred on the cedar wood samples due to the combined effect of these modifications were evaluated by measuring their wettability and colour and using attenuated total reflection Fourier-transform infrared spectroscopy (ATR-FTIR) and X-ray photoelectron spectroscopy (XPS) analyses. The surface analysis by XPS showed the expected variability among the sampled layers for unmodified and thermally modified cedar wood samples and a uniform composition after the AKD coverage, regardless of their pre-treatments. The FTIR spectra before the irradiation test showed that the hydrophobicity of the samples was ensured by the formation of carbonyl groups originating from the reaction between the AKD and hydroxyl groups of cellulose, which is related to the presence of the absorption band between 1700 cm^{-1} and 1750 cm^{-1}. Markedly, after the irradiation test, a degradation of the amorphous cellulose component occurred, showing that photoisomerisation to the enolic form took place. Overall, although uniform AKD coverage was derived from the surface analysis and wetting test, the combined ATR-FTIR results and colour measurements showed that it could not provide permanent protection to the underlying wood structure due to its own tendency to degrade mainly in colour over time, under the action of UV rays and atmospheric agents.

Keywords: deodar cedar; wood surface; thermo-vacuum modification; alkyl ketene dimer; hydrophobic effect; XPS

Citation: Lovaglio, T.; D'Auria, M.; Gindl-Altmutter, W.; Giudice, V.L.; Langerame, F.; Salvi, A.M.; Todaro, L. Thermal Modification and Alkyl Ketene Dimer Effects on the Surface Protection of Deodar Cedar (*Cedrus deodara* Roxb.) Wood. *Forests* **2022**, *13*, 1551. https://doi.org/10.3390/f13101551

Academic Editors: Miha Humar, Roberto Zanuttini and Francesco Negro

Received: 21 August 2022
Accepted: 19 September 2022
Published: 22 September 2022

1. Introduction

In recent years, a major problem for the wood-processing industry is the insufficient amount of wood raw materials on the local market, which results in increased competition between companies and producers of wood-based products. This competition is expected to become even more intense due to the constantly increasing global demand for wood and wood-based materials. Consequently, timber prices have also been rapidly rising. These recent changes are leading to serious supply chain problems with likely slowdowns occurring in the production of wooden products. Thus, the continuous and sustainable supply of wood raw materials is of central importance for the smooth functioning of the wood-processing industry [1]. In this context, the recovery and optimised utilisation of local, underused wood species represents a viable option for reducing the negative

economic impact that is caused by the unstable wood supplies from abroad. Better handling of underused local wood resources could be crucial for meeting the increased demands of the wood sector, keeping in mind that the sustainable management of the wood resources could bring the consequential development and improvement of the national economy [2].

Wood has traditionally been used in many value-added applications due to its numerous outstanding properties. However, being a natural material, it is also characterised by several disadvantages that are related to the great variability in its properties. Wood is a biodegradable, natural material and is permanently exposed to the degradation processes of environmental, chemical, physical, and microbiological origin. Wood materials undergo photodegradation and change their colour irreversibly in response to light and water [3]. Due to water absorption and desorption, wood is easily subjected to biological attacks by fungi and insects or swelling and shrinkage changes. All of these effects constitute a negative impact on the performance properties of wood materials, especially when they are used outdoors.

Deodar cedar (*Cedrus deodara* Roxb.) of the *Pinaceae* family was largely planted in the past mainly as an ornamental tree that was grown in parks and gardens, but it was also planted for reforestation purposes.

In favourable conditions, it grows rapidly, up to 40–50 m tall, and it reaches more than 100 cm in diameter, from terrain that spans from the sea to the mountain level. The sapwood is pink or greyish and differs from the reddish/yellow heartwood. Deodar wood exhibits low hardness and high durability mainly in the heartwood. Gum-resinous exudations are also frequent. It is a durable and rot-resistant wood that is used as a construction material in naval construction, furniture, sculptures, temples, etc. [4]. Cedar wood is known for its excellent machining properties, as well as an impressive strength-to-weight ratio. The physical and mechanical properties of cedar wood have often been reported under the genus Cedar with there being no distinction between species. In [4], the compression, the bending strength, and Modulus of Elasticity (MOE) of it were 49 N/mm^2, 94 N/mm^2, and 10,100 N/mm^2, respectively. Its density, at the 12% of moisture content, was 0.52 g/cm^3. In terms of its durability, the wood is classified as a three on the scale, which means that it is moderately resistant [5].

However, deodar cedar is still one of the less-studied wood species in the field of wood modification and surface behaviour. A recent paper highlighted the influence of the thermal modification process on the wood's machinability [6], while the effect of solvent on the extractive contents was analysed by Lovaglio et al. [7]. Some studies on the effect of heat treatments on the physical, mechanical, and chemical properties of cedar were conducted by Nabil et al. [8], while Bal et al. [9] reported the effect of thermal modifications on the physical properties of *Cedrus libani* wood.

The treatment of the cedar wood surface by the combination of spores (*Penicillium expansum* and *Penicillium commun*) was also studied, thereby highlighting the evolution of the physicochemical properties of the wood surface before and after the adhesion of fungi [10]. In addition, interesting results in terms of its physicochemical surface properties were obtained by using a cellulase treatment [11]. The same article pointed out that, before the cellulase treatment, the untreated cedar surface appeared, at first, to be hydrophobic and then the hydrophobicity decreased continuously until it reached a state of hydrophilicity.

These results have induced us to perform further studies on the relationship between durable wood species and wettability considering that, as it was reported in previous papers, the correlations between wettability and durability have not been completely clarified [12]. In addition, the extractive compounds are recognised to be the most important factor in determining the durability of the wood, although the extractive concentration does not necessarily correspond to natural durability [13,14]. Generally, durable wood from which extractives are removed, e.g., due to thermal modification, could become susceptible to decay [14] or they may change its wettability [15].

The thermal modification of wood is a method that enhances certain critical properties of wood, although some drawbacks in its mechanical properties are highlighted [16]. Concerning the effect of thermal modifications on wettability, the results are not always consistent [17]. Recently, several researchers highlighted that thermal modification changes or modifies the nature of the extractives, and consequently, it affects the wettability of both durable and nondurable wood species.

To enhance the performance of wood under critical environmental conditions, different approaches may be applied. Most wood preservatives produce toxic emissions during their production and service life [18].

The positive effect that alkyl ketene dimer (AKD) has on rendering wood surfaces hydrophobic has already been recognised [19–21]. The characteristics and the action mechanisms of AKD have been discussed in a previous research paper [22]. In that paper, numerous methods (based on the use of fluorine, and octadecyltrichlorosilane, among others) to render wood materials water-repellent were also presented.

The treatment of fluorination, based on the substitution of –OH hydrophilic groups by covalent carbon–fluorine bonds, decreased the hydrophilicity of the wood [23]. Hui et al. [24] demonstrated that an octadecyltrichlorosilane treatment made the wood surface hydrophobic, also, under prolonged exposure of UV light or rain.

To the best of our knowledge, no studies have reported on the effect of thermal modifications when they are combined with the application of AKD on cedar wood properties, before and after an irradiation test. In addition to the usual techniques (wettability, colour, and FTIR) we used an XPS, a surface-specific technique, to investigate the chemical state of the elements constituting the outermost layers of the wood samples and their relative variation due to the combined surface treatments.

2. Materials and Methods

2.1. Sample Preparation

The wooden boards of 40 mm (tangential) × 200 mm (radial) × 2200 mm (longitudinal) were obtained from four trees that were nearly 70 years old, which were cut down in a high regional forest located in the region of Basilicata, Southern Italy, and then, they were thermally modified as explained below.

2.1.1. Thermal Modification

Before the thermal modification, the boards were conditioned at a temperature of 20 °C and relative humidity of 65%. The heat was applied to the boards by us gradually increasing the temperature to 200 °C, under a pressure condition of 220–320 mbar for 4 h in a thermo-vacuum cylinder (WDE-Maspells.r.l., Terni, Italy). The wood density before and after the thermal modification was 0.480 and 0.416 g/cm^3, respectively. Further information on this technology was previously described by Ferrari et al. [25].

2.1.2. Irradiation Test

The UV test was carried out according to the EN 927–6 standard [26], and the experiment lasted for one week. The cycle started with 24 h of conditioning, followed by 2.5 h UV exposure, and then 0.5 h of water spraying. In total, the samples were put in chamber test for 116 h, i.e., 24 h conditioning + 15 h spraying water + 77 h UV irradiation. The apparatus was equipped with UVA 340 nm lamps which were maintaining a constant temperature of 45 °C during the conditional phase and 60 °C during the UV irradiation. The irradiation set point was 89 W/m^2 at 340 nm and the conditions during the spray phase varied from 6 l/min to 7 l/min during the period when the UV light was off.

2.2. AKD

Twenty-four cedar wood samples without defects were used for conducting the experiment. The dimensions of the samples were 5 mm × 50 mm × 50 mm in the tangential, radial, and longitudinal directions, respectively. The samples were immersed in three different AKD/toluene solutions for 10 s each (see Lovaglio et al. for further details [22]). The AKD solutions were obtained by dissolving AKD wax C18 in toluene solvent to achieve: 0.1%, 5%, and 10% concentrations (*w*/*w*). Then, the samples were put under a fume hood where the toluene was allowed to evaporate overnight. Finally, the samples were kept at a standard climate of 20 °C and 65% relative humidity.

The samples were then randomly assigned to groups according to Table 1.

Table 1. Experimental design of unmodified and thermally modified cedar wood samples for the different solutions of alkyl ketene dimer (AKD) (% *w*/*w*). C*TH= thermally modified. C= unmodified.*

Treatment	Pre-UV Test	Post-UV Test
	Cedar Code Abbreviation	Cedar Code Abbreviation
Unmodified	C	C post-UV
TH	CTH	CTH post-UV
Unmodified + 0.1% AKD	C + 0.1% AKD	C + 0.1% AKD post-UV
CTH + 0.1% AKD	CTH + 0.1% AKD	CTH + 0.1% AKD post-UV
Unmodified + 5% AKD	C + 5% AKD	C + 5% AKD post-UV
CTH + 5% AKD	CTH + 5% AKD	CTH + 5% AKD post-UV
Unmodified + 10% AKD	C + 10% AKD	C + 10% AKD post-UV
CTH + 10% AKD	CTH + 10% AKD	CTH + 10% AKD post-UV

2.3. Water Contact Angle (WCA)

The water contact angle measurement [27] was determined using the Drop Shape Analyzer-DSA30 (KRŰSS, Hamburg, Germany). A 7.5 μL distilled water drop was applied on the surface, utilising a digital pipette WCA. The image of the liquid drop was captured using a high-resolution camera and transferred to a computer screen where the contact angle was measured using ADVANCE software (KRŰSS, Hamburg, Germany). The image was captured immediately after the water drop was applied (0 s.), and then every 0.5 s for a total time of 2 min. Each WCA measurement was made 3 times on each of the 24 wood specimens, before and after the irradiation test.

2.4. ATR FTIR Spectroscopy

The wood samples with the dimensions of 5 mm × 50 mm × 50 mm in the tangential, radial, and longitudinal directions, respectively, before and after the irradiation test, were analysed by using ATR-FTIR spectrometry. ATR-FTIR spectroscopy is the study of the interaction of electromagnetic radiation with matter; the spectrum that is obtained indicates the molecular vibration. When they are exposed to infrared radiation, sample molecules selectively absorb the radiation of specific wavelengths which causes the change of the dipole moment of the sample molecules. The commonly used region for infrared absorption spectroscopy is from 4000 cm^{-1} to 400 cm^{-1} for most organic and inorganic compounds.

The spectrometer that was used during this study was attenuated total reflectance-Fourier transform infrared spectroscopy—PerkinElmer, FT-IR Spectrometer Frontier (Perkin Elmer Inc., Waltham, MA, USA). The instrument was equipped with Spectrum™ software (Perkin Elmer Inc., Waltham, MA, USA) which was operating on 4 scans and 2 cm^{-1} resolutions. The spectra were recorded within the wavelengths from 650 cm^{-1} to 4000 cm^{-1}. The software connected to the spectrometer was able to correct the baseline and normalise the spectra. To normalise the infrared spectra, the band which was referred to as 1025 cm^{-1}

in the fingerprint region was used. For the samples with AKD, the band that was usually used was at 2917 cm^{-1} [22].

2.5. Colour

The colour changes during the ageing process were constantly monitored on the specimens, based on the method of the Commission International de l'Eclairage (CIE) using colour parameters, *L**, *a**, and *b** and their average values were calculated for each treatment. CIEL*a*b* is one of the models that better showed a uniform colour spacing in their values. CIEL*a*b* indicated these values with three axes: *L**, *a**, and *b**, which made distinctions between light and dark, red and green, and blue and yellow, respectively. The three coordinates of the CIEL*a*b* represent: the central vertical axis, which is the lightness (*L**) whose values run from 0 (black) to 100 (white); the axis *a** which makes distinctions between the red/magenta and green colours. The values that are negative for *a** indicate the presence of green, while the positive values indicate the presence of magenta; the values of axis *b** represent the presence of yellow and blue. The values that are negative for *b** indicate the presence of blue, and the positive values indicate the presence of yellow [28].

The instrument that was used to observe the colour of the samples and their variations was the Konica Minolta CM-2002 spectrophotometer (Konica Minolta Inc., Tokyo, Japan). It was equipped with a pulsed Xenon arc light source that was employed with a measurement area of 8 mm in diameter on the samples. Colourimetric measurements were also performed on three separate locations and repeated three times before and after the thermal modification and AKD treatment. Furthermore, the measurements were repeated after the irradiation test. The Δ values were calculated by comparing the modified samples with the untreated ones, considering the different solutions of AKD that were used. The statistical significance of the differences in the colour coordinates were then investigated using an analysis of variance (ANOVA) together with a Tuckey test. All of the statistical analyses were conducted using SPSS Statistics software v.11 (SPSS Inc, Chicago, IL, USA).

2.6. X-ray Photoelectron Spectroscopy (XPS)

XPS is also known by the acronym ESCA (Electron Spectroscopy for Chemical Analysis), and the acquired spectra are susceptible to multiple levels of interpretation, ranging from a simple qualitative evaluation of the elements that compose the specimen to the determination of their chemical state and the semi-quantitative analysis [29]. XPS is a surface-sensitive technique whose sampling depth is in the order of nanometres due to the use of electron inelastic mean free paths. Only the electrons that are emitted by the atoms of the outer layers can escape from the sample surface with an unchanged kinetic energy and contribute to the photoelectron signals that are detected by the analyser of the spectrometer.

The first step that was taken in characterising the surface chemistry of the specimen that was under investigation was the identification of the elements that were present, i.e., a qualitative analysis. For this purpose, usually, a wide spectrum is recorded over the whole energy region that is allowed by the XPS source, which will provide various intense signals to be identified using the software that is supplied with the spectrometer that is in use. The second step of XPS, one of its major strengths, is based on its ability to determine the chemical state of the identified elements constituting the sample. Usually, the "detailed" spectra of the signals of interest are registered with a resolution in energy that is ten times higher than that which is used for the wide spectra. In this way, it is possible to appreciate the peak displacement due to the oxidation state of atoms that are taken into account. The shift that occurs depends on the charge of the atom, and chemical assignments can be performed by referring to a standard analysis, data that are reported in the literature [30,31], and an online database [NIST XPS 20, Version 4.1, 2012: https://srdata.nist.gov/xps/default.aspx, accessed on 23 April 2022].

Unlike many other surface sensitive techniques, XPS allows for semi-quantitative mass balances. The intensity of the signals is directly proportional to the number of atoms that are chemically equivalent in the sample, therefore, in measuring the area of the peaks,

it is possible to evaluate their relative abundance, after a normalisation procedure [22,23]. For complex systems, particularly when using achromatic sources, like the wood samples that are examined in this work, it is fundamental to properly resolve the closely spaced chemical states by an accurate curve-fitting procedure. In this work, the curve-fitting software *NewGoogly* was employed, which allows for estimating the intrinsic and extrinsic contributions of the XPS spectra [32,33].

XPS spectra were acquired using a SPECS Phoibos 100-MCD5 spectrometer (SPECS Surface Nano Analysis GmbH, Berlin, Germany) that was operating at 10 kV and 10 mA and in the medium area (diameter = 2 mm), using the MgKα (1253.6 eV) and AlKα (1486.6 eV) radiations. The pressure in the analysis chamber was less than 10^{-9} mbar during the acquisition. The wide spectra were acquired in FAT (Fixed Analyser Transmission)/FRR (Fixed Retarding Ratio) modes that were E^0 = 20 eV/R = 30, and channel widths of 1.0 eV. Little wood specimens with the dimensions of 15 mm × 5 mm × 5 mm in the tangential, radial, and longitudinal directions, respectively, were used for this purpose.

Detailed spectra were all acquired in FAT mode with a constant pass energy E^0 of 9 eV and channel widths of 0.1 eV and were curve-fitted using the well-established procedure (*NewGoogly* software) [32,33]. Peak areas and positions (binding energies, BEs) as derived by the curve-fitting were, respectively, normalised using proper sensitivity factors and referenced to C1s aromatic/aliphatic carbons as the internal standards, respectively, were set at 284.8/285.0 eV [30,31].

3. Results and Discussion

3.1. Water Contact Angle (WCA)

This study investigated the effect of weathering on the WCA of untreated and thermally modified wood with or without AKD. The results of the WCA measurements are shown in Figures 1 and 2.

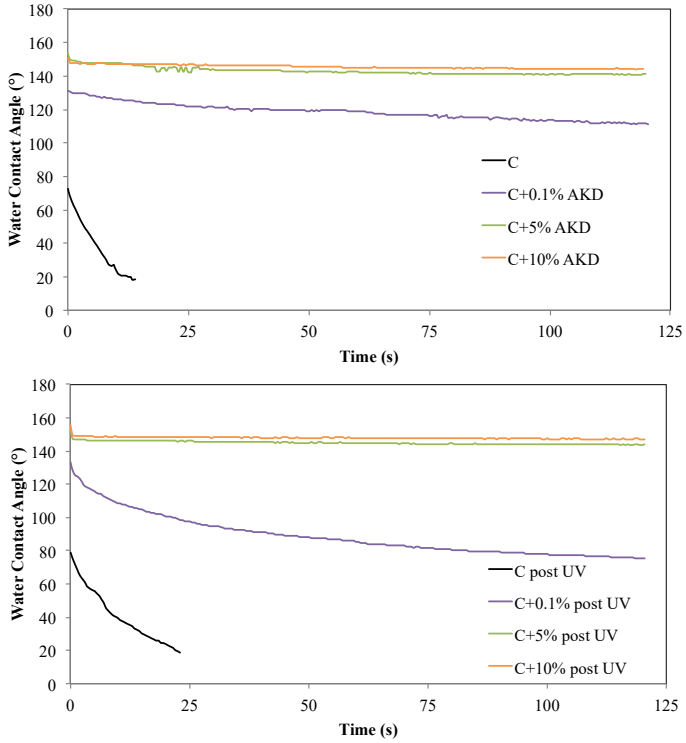

Figure 1. WCA values over time on cedar wood samples, before (**top**) and after the UV treatment (**bottom**).

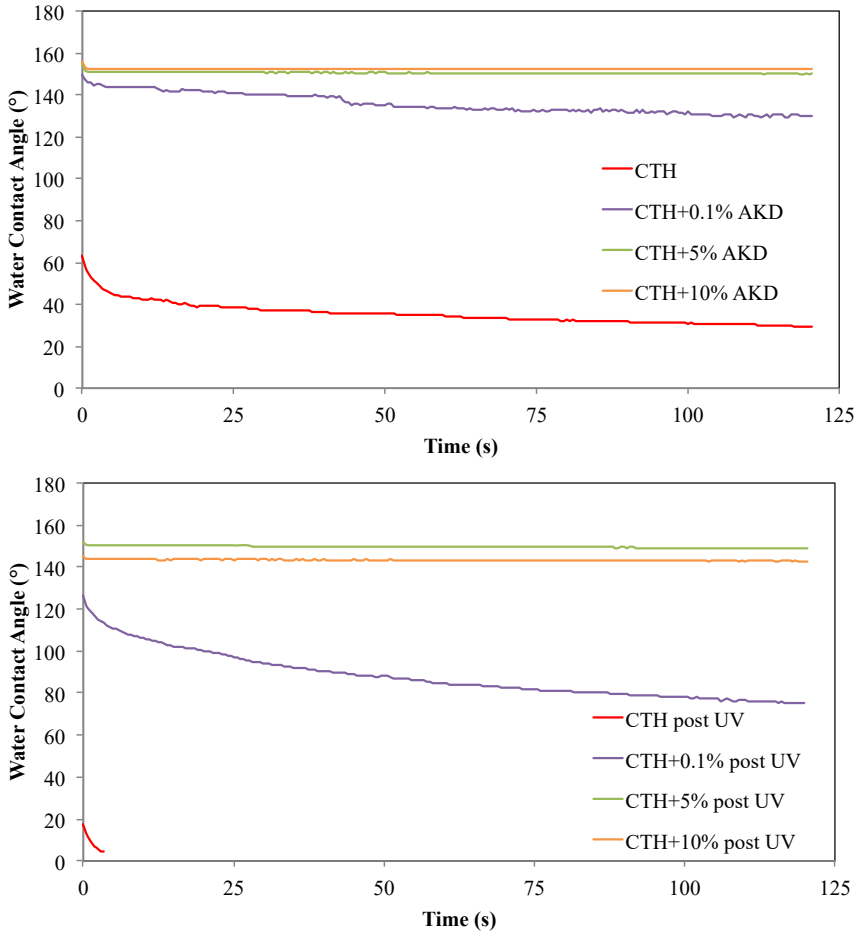

Figure 2. WCA values over time on thermally modified cedar wood samples, before (**top**) and after the UV treatment (**bottom**).

According to Vogler [34], when the value of the WCA exceeds 65°, the surfaces are characterised as hydrophobic. Inversely, with WCA that is less than 65°, the surfaces are considered to be hydrophilic.

As expected, the water was absorbed faster by the untreated wood (C, Figure 1, top) than it was by the thermally modified wood samples (CTH, Figure 2, top). The lower wettability on the wood surface after the thermal modification could be the result of several phenomena that are taking place in the wood. One cause could be the migration of extractives to the surface during its heating [35]. Extractive compounds can be polar and non-polar compounds, and the migration to the surface of the high content of non-polar extractives is considered primarily responsible for the low wettability that is recorded [36].

As it will be shown in the next sections by the completion of surface (XPS) and infrared (ATR-FTIR) spectroscopies, several events are recognised to also play an important role on the reduced hygroscopicity of the wood surfaces. Different types of reactions between the cell wall components occurred during heating and they implied a cross-linking between the lignin and polysaccharides, and a reduction in free hydroxyl groups [37]. At high temperatures, the hemicelluloses can undergo oxidation and pyrolysis reactions with consequent changes in compounds like furfural polymers, which are considered to be less hygroscopic [38]. The hydrophobicity of both C and CTH was greatly improved after the application of AKD, and all of the samples that were treated with a different AKD solution exhibited a steady water contact angle of approximately 140°–150° (Figures 1 and 2, top).

The hydrophobicity of the surface may be caused by the esterification reactions between the AKD and wood compounds such as cellulose [19].

Arminger et al. [21] conducted a study on European beech (*Fagus sylvatica* L.) wood surface and they used eight different dispersions with target AKD concentrations of 1 or 10 g L^{-1} water. Depending on the specific conditions of the application, the water contact angles that were as high as 166° were measured on the treated wood surfaces.

As suggested by Shi et al. [39], the greatly increased hydrophobicity of the AKD-modified cedar wood may be due to the introduction of long alkyl chains from the AKD on the cellulose surfaces via ketoester linkages; these directly react with hydroxyl groups from cellulose to form β-ketoester linkages by esterification. They also stated that the improved hydrophobicity of the wood could be attributed to a reaction between the wood and the AKD that formed β-ketoester linkages. However, some researchers disagree about whether or not AKD is covalently bonded to cellulose [39]. After the irradiation test, an increased wettability of the thermally modified wood samples was determined, and the contact angles of the CTH decreased significantly (Figure 2, bottom). This result is similar to those of other published works [40], and it was attributed to the combination of structural and chemical changes on the woods' surfaces [37,40].

The application of AKD solutions at 5% and 10% positively affected the wettability, thereby making it unchanged for both the C and CTH wood surfaces, and also after the irradiation test. In contrast, for the sample that was treated with a 0.1% solution of AKD, a significant decrease in the WCA was observed, though the wood surface remained hydrophobic.

Markedly, the wettability of the C and CTH decreased significantly after the irradiation; furthermore, no difference between the C + AKD and CTH + AKD could be distinguished, and the water contact angled of the wood surface were similar, with a steady angle of approximately 150°, except for the C + 0.1% AKD and CTH + 0.1% AKD samples, where a slight reduction of the angle was observed. Similar results were found in the study by Yan et al. [20] where the variant of a hydrophobised microfibrillated cellulose (MFC) at the lowest concentration of AKD gave a slight reduction in the water contact angle during the two minutes of the measurement time, thus indicating the slight penetration of water into the MFC pellets.

3.2. ATR-FTIR Analysis

The characteristic peaks of AKD were located at the wave numbers of 2915 cm^{-1} and 2848 cm^{-1}, which were the C-H stretching vibrations representing the methyl and methylene groups of the alkyl chain in the AKD molecule (Figure 3). The peak at 1848 cm^{-1} is related to the stretching of C = O, while the peak at 1700 cm^{-1} is related to the group C = C.

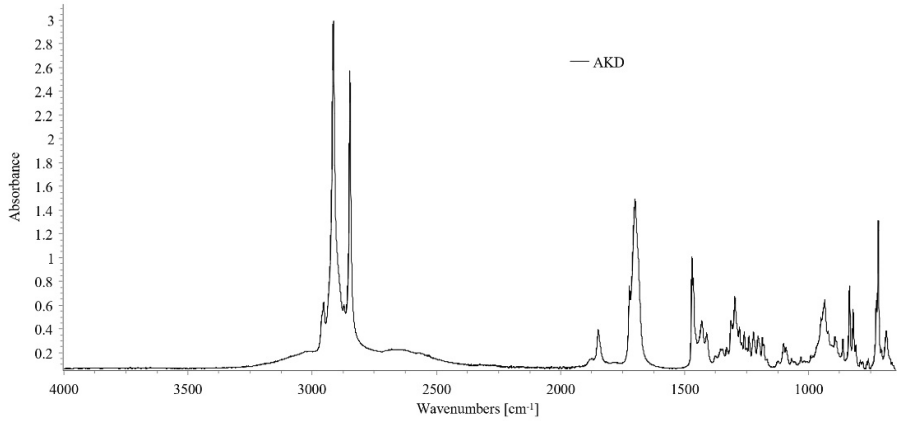

Figure 3. FTIR spectra of AKD wax [22]. Reprinted from Teresa Lovaglio (2019).

Figure 4 shows small but significant spectrum changes between C and CTH, i.e., the decrease of the peak at 1610 cm^{-1} after heating. This indicated the degradation of the guaiacyl unit of lignin [41,42]. The band at 1734 cm^{-1}, which is assigned to the C = O stretching vibration of acetyl or carboxylic acid, highlighted a peak that was slightly smaller in CTH due to the cleavage of the acetyl side chains in the hemicelluloses [43]. Figure 5 shows the significant changes that occurred after the irradiation process of the bands at 1595 cm^{-1}, 1510 cm^{-1}, and 1465 cm^{-1}, indicating lignin degradation. The decrease of the bands at 1595–1510 cm^{-1} showed that the guaiacyl nuclei were sensitive to the artificial ageing degradation process. In contrast with the results that were reported by Hon [44], the absorbance to stretching vibration of the carbonyl in the 1,3-ketoester at 1730 cm^{-1} greatly decreased.

Only the fingerprint region of the FTIR spectra of C and CTH, pre and post UV, are highlighted in Figure 6 to better illustrate the impact of UV irradiation on wood surfaces.

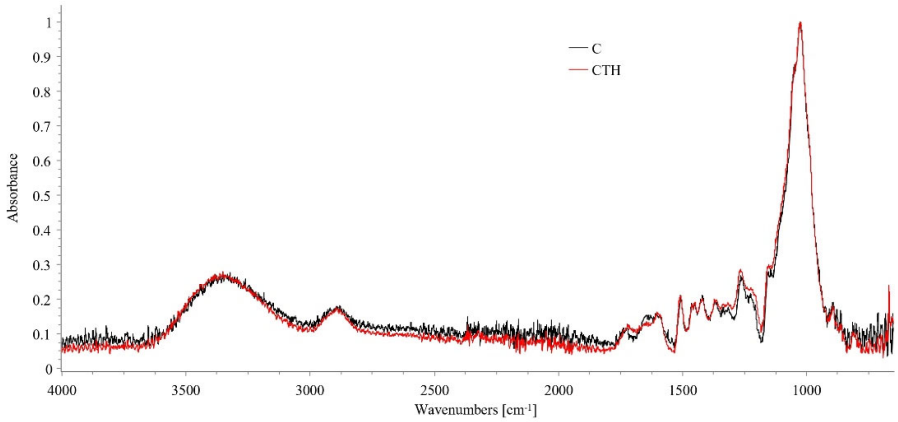

Figure 4. Comparison of FTIR spectra of cedar wood samples before and after the thermal modification (C and CTH).

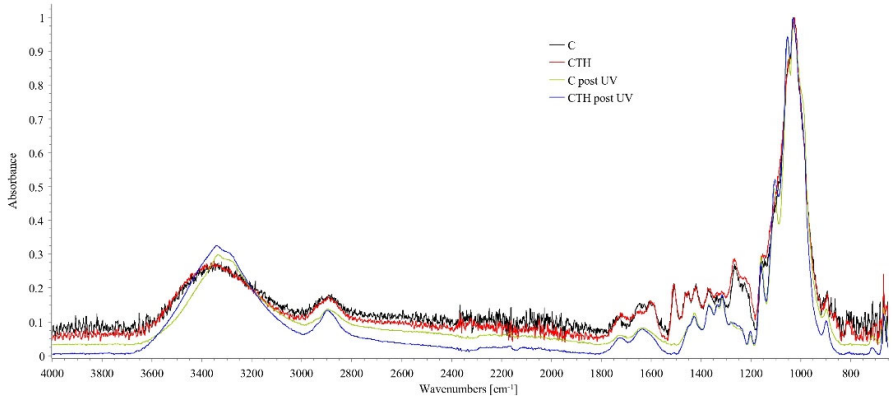

Figure 5. Comparison of FTIR spectra of C and CTH pre- and post-UV treatment.

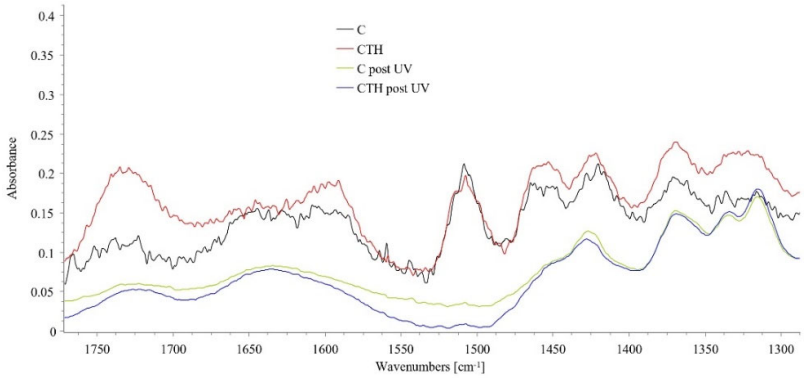

Figure 6. Comparison of FTIR spectra of unmodified and thermally modified cedar wood samples, pre-and post-UV treatment, in the fingerprint region.

After the UV irradiation, the development of the two peaks at 1335–1316 cm^{-1} were observed and were attributed to the cellulosic crystal content. During the irradiation test, the degradation of the amorphous cellulose component was depicted. The band related to CH_2 stretching was shifted at 1430 cm^{-1} due to the degradation of amorphous cellulose, and this was also the case for the cedar wood samples. The investigation of C + AKD and CTH + AKD, with different concentrations of AKD solutions, is shown in Figure 7.

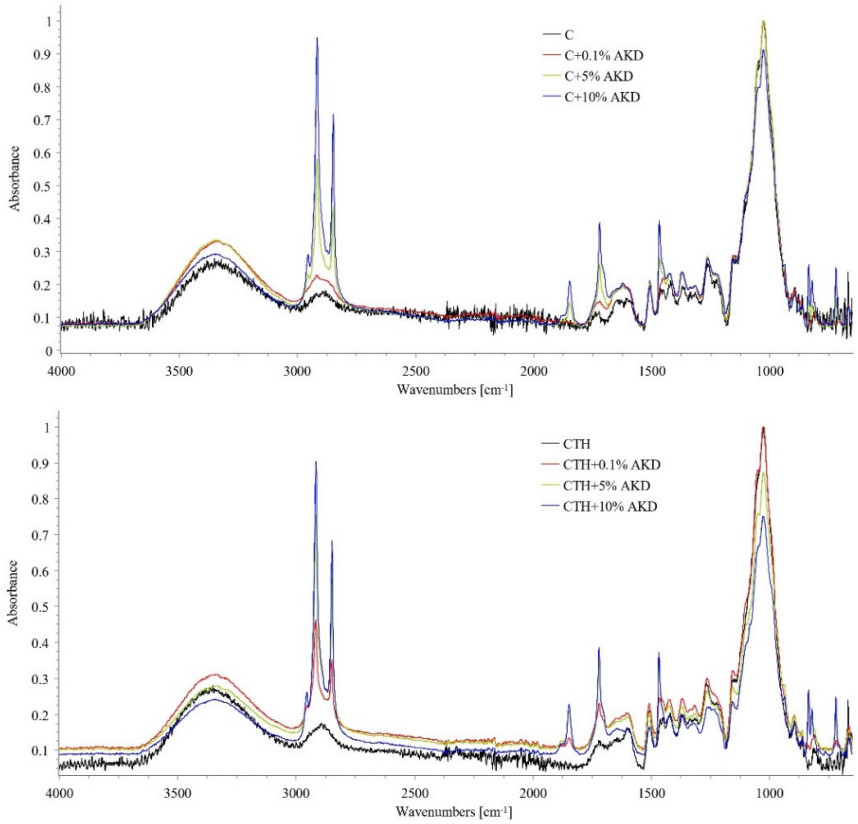

Figure 7. Comparison of FTIR spectra of unmodified (**top**) and thermally modified cedar wood samples (**bottom**) with AKD.

The reaction between the AKD and wood fibre hydroxyl groups of cellulose was identified by the absorption band at 1720 cm^{-1}. In previous research, Hubbe [19] reported that the reaction mechanisms of AKD with wood fibre hydroxyl groups of cellulose were

considered as an esterification reaction. As expected, important differences in the intensity of the bands between the different concentrations of AKD occurred. In the case of the concentration of 0.1% AKD, contrary to Alder [22], the peak at 1720 cm^{-1} was more intense for CTH compared to that of C, thus highlighting that thermal modification induced a better condition of bonding between wood fibre and AKD. The thermal modification changed some of the chemical components of the cell walls by a depolymerisation-induced process [37,40] that may produce new binding sites with the AKD molecule. Yan et al. [20], in a research study on hydrophobised microfibrillated cellulose that was characterised by Fourier transform infrared spectroscopy, nuclear magnetic resonance, and an X-ray analysis, found strong indications for the presence of AKD on the surface before and after its extraction with solvent. Nevertheless, only a very small amount of covalent β-ketoester linkages, between the modification agent and cellulose, were identified. No scientific evidence has been found that deals with the combination of thermal modification and other findings concerning the AKD.

After the weathering test, relevant changes were observed (Figure 8). The peaks at 2915 cm^{-1} and 2848 cm^{-1} are related to the C-H stretching vibration, representing the methyl and methylene groups of the alkyl chain in the AKD (see also Figure 3). After irradiation, a lower intensity of the spectra in the C + AKD sample after the UV procedure was highlighted, compared to that of the CTH + AKD sample after the UV procedure. At the peak at 1730 cm^{-1}, the carbonyl absorption of the 1,3-ketoester almost disappeared, thereby showing a photochemical tautomerisation in favour of the enolic form (Scheme 1). The effect of light on the tautomeric equilibrium is well known [45–47]. Usually, photochemical isomerisation induces an increase in the ketonic form. To our knowledge, this is the first experimental result where UV irradiation induced a sharp reduction of the ketonic form.

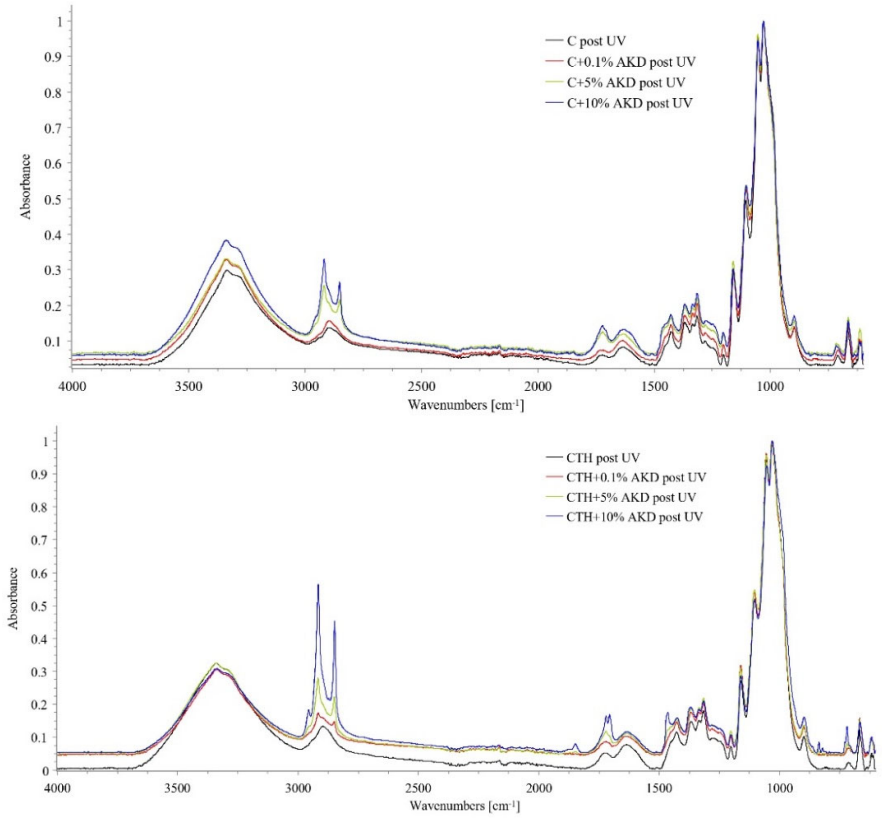

Figure 8. Comparison of FTIR spectra of unmodified (**top**) and thermally modified cedar wood samples (**bottom**) with AKD after the UV irradiation test.

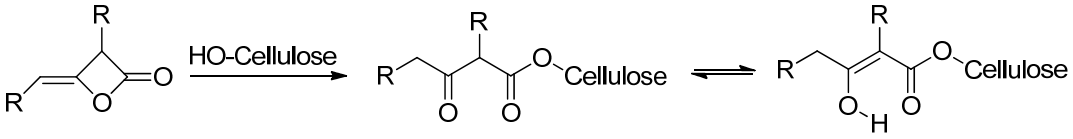

Scheme 1. The reaction of AKD with cellulose.

3.3. Colour

The results that were obtained for the colour changes of both the unmodified and thermally modified deodar cedar wood samples after the application of AKD are presented in Table 2.

Table 2. Colour change (mean value) for both unmodified and thermally modified cedar wood samples after the AKD application. *Means with the same letter are not significantly different from each other (p > 0.05 ANOVA followed by Duncan test).*

	Δ*L*	**Δ*a***	**Δ*b***	**Δ*E***
Unmodified samples				
C	0	0	0	0
C + 0.1% AKD	0.36 ^{a}	−0.35 ^{a}	−2.27 ^{c}	2.40 ^{a}
C + 5% AKD	1.77 ^{b}	−0.44 ^{b}	−1.86 ^{b}	2.95 ^{b}
C + 10% AKD	2.69 ^{c}	0.47 ^{b}	−0.40 ^{a}	2.97 ^{b}
Thermomodified				
CTH	−22.64 ^{b}	2.21 ^{c}	−1.43 ^{b}	22.81 ^{c}
CTH + 0.1% AKD	2.52 ^{a}	−0.50 ^{b}	1.56 ^{b}	3.03 ^{a}
CTH + 5% AKD	2.75 ^{a}	−1.90 ^{a,b}	−9.8 ^{a}	10.40 ^{b}
CTH + 10% AKD	2.12 ^{a}	−2.28 ^{a}	−11.21^{c}	11.65 ^{b}

As reported by several authors [17], the first step is the darkening (L^*) of wood surfaces after their thermal modification (Table 2). The change in the natural colouration of the wood and in particular, the darker tonality after its heating can be attributed to the chemical reactions of oxidation or the formation of a new compound by the degradation of the wood's components [48,49].

Extractives of each wood species make a specific colour which is expressed by two chromatic parameters, namely a^* and b^*. The redness coordinate a^* increased during the heat treatment (2.21). The change in b^* (−1.43) was particularly influenced by the reactions that involved the lignin and lignin derivates, such as quinone and stilbenes [50].

After the immersion of each sample in the AKD solutions, the relevant variations in ΔE (11.65 for and CTH + 10% AKD) were observed. The colour change was mostly due to modification of the L^* coordinate and b^* coordinate. The greying of the surfaces was caused by the natural colour of AKD. The wax is white in the solid phase, and the solution results were transparent but, probably, when the solvent flew off under the fume cupboard, a grey layer had been created on the surface. Increasing amounts of deposited AKD wax affected the optical properties of the wood surface, thus producing an increase in the colour change, as expressed by ΔE. Also, Arminger et al. [21] conducted a study on European beech wood surface and they showed a gradual lightening from the native reddish beech wood colour to a whitish surface. The implementation of sub-microstructures clearly reduced the surface gloss, but the transparency and colour of the wood remained largely unchanged [21].

The colour changes of the specimens that occurred after the irradiation test are displayed in Table 3.

Table 3. Colour changes (mean value) for both unmodified and thermally modified cedar wood samples with AKD after UV irradiation. *Means with the same letter are not significantly different from each other (p > 0.05 ANOVA followed by Duncan test).*

Cedar Post-UV	Δ*L*	Δ*a*	Δ*b*	Δ*E*
Unmodified samples				
C	−7.50 ^{b}	1.73 ^{b}	−0.80 ^{a,b}	8.01 ^{a}
C + 0.1% AKD	−9.39 ^{b}	1.32 ^{a}	−1.54 ^{a}	9.63 ^{a,b}
C + 5% AKD	−11.17 ^{a}	1.57 ^{a,b}	−0.95 ^{a,b}	11.42 ^{b}
C + 10% AKD	−8.91 ^{b}	1.70 ^{b}	−0.14 ^{b}	9.40 ^{a,b}
Thermomodified				
CTH	5.80 ^{b}	−2.23 ^{a,b}	−5.36 ^{b}	8.23 ^{b}
CTH + 0.1% AKD	5.75 ^{b}	−3.20 ^{a}	−9.2 ^{a}	11.35 ^{b}
CTH + 5% AKD	2.66 ^{a}	−1.56 ^{b}	1.30 ^{c}	3.69 ^{a}
CTH + 10% AKD	3.53 ^{a,b}	−1.43 ^{b}	4.23 ^{d}	5.75 ^{a,b}

The energy that is associated with the UV light region is sufficient to break many bonds that are present between the chemical components of wood [51]. The effect of weathering on wood surfaces has been investigated, extensively [22,49–51], and similar to the results of these studies, the Δ*E* values of the C samples depended mainly on Δ*L* (Tables 2 and 3). The colour of the wood surface changed rapidly from light to dark and this was indicated by a decrease in Δ*L* (7.50).

After a thermal treatment, the darker wood colours are attributed to the development of oxidation products like quinones [50]. Sadly, it has been shown that the colour of thermally treated wood fades when it is exposed to light.

In fact, in a study by Miklecic et al. [52], the FTIR spectra of wood samples that were subjected to UV light showed that exposure to UV light induced a decrease in the lignin-related peaks (delignification) of the samples.

In general, during the interaction with light, the lignin reacts with oxygen and free radicals thus producing chromophoric groups that are responsible for the darkening of the surfaces. Therefore, photo-discolouration and photo-degradation [51] occurred also in the AKD-protected samples.

3.4. XPS Analysis

The wood samples were properly sized to be mounted on the XPS sample holder and the analyses were performed on the unmodified and thermally modified wood surfaces (Figure 9).

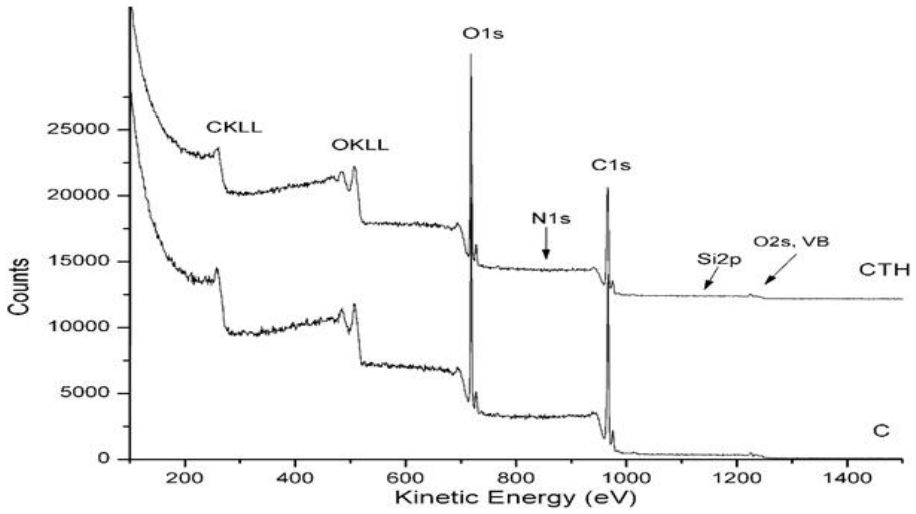

Figure 9. Wide spectrum of thermally modified (CTH, **top**) and unmodified cedar wood samples (C, **bottom**).

The labelled wide spectra showed that carbon and oxygen were the main elements. Traces of silicon and nitrogen could only be perceived by amplifying the relevant KE zones. In fact, after the acquisition of the spectra at a higher resolution, the detail regions confirmed that the silicon signals were at the limit of detection for both samples, and just a very small percentage of nitrogen could be quantified only for the CTH sample. All of the detailed regions whose areas could be resolved via a curve-fitting were considered for the compositional analysis of both samples (vide infra). As mentioned in previous work [53], the degradation of wood during heating can be detected with XPS by a change in the atomic ratio of the main elements. Thus, also in this work, to monitor the chemical modifications of the wood after thermal treatments, the C1s and O1s regions of C and CTH cedar samples were especially regarded, and their O/C ratios were compared.

The curve-fitted C1s regions of the C and CTH samples are compared in Figure 10.

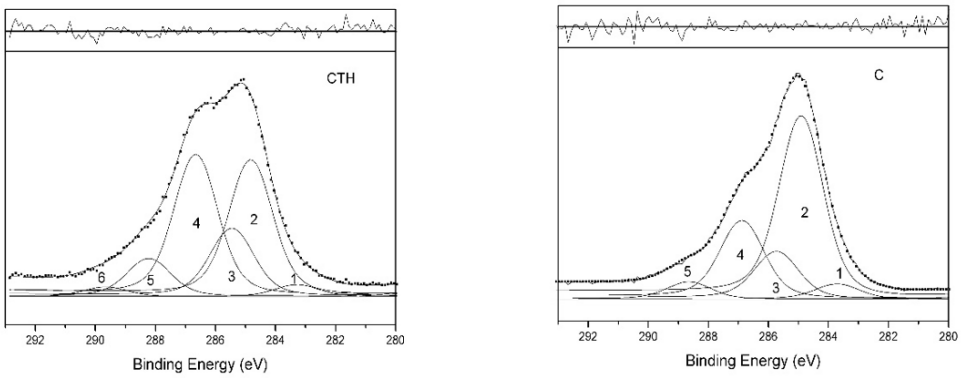

Figure 10. C1s curve-fitted regions of thermally modified (CTH) and unmodified (C) cedar wood samples.

Table 4 lists the corrected binding energies (BEs) and normalised areas of the resolved peaks, including the curve-fitting results from other detailed regions of both of the cedar samples. The choice for the best curve-fitting was based on the satisfactory mass balance of the carbon-containing oxygen components and the total O1s area, taking into account the stoichiometric coefficients and the limit of the XPS accuracy (±10%) [30,31]. The peak parameters were imposed to be the same within each region to facilitate this computation, as was also conducted in previous work [53], and the 'residuals' were reported on top of

the curve-fitted figures to testify the goodness of this approximation. The chemical state assignments that are detailed below are based on previous work [53], the NIST XPS database, and the literature data.

Table 4. Fitting parameters of the C1s, O1s, and N1s detailed regions for both the CTH and C samples.

Region	Peak Number	C		CTH	
		Binding Energy (BE) (Ev)	Norm. Area (a.u.)	BE (Ev)	Norm. Area (a.u.)
C_{1S}	1	283.6	1861.2	283.3	1194.2
	2	284.8	22,246.1	284.8	13,621.0
	3	285.6	5806.5	285.4	6813.1
	4	286.7	9550.4	286.6	14,162.4
	5	288.5	2120.6	288.2	3797.9
	6	-	-	289.6	975.24
O_{1s}	1	532.0	1753.4	531.6	2044.9
	2	533.0	12,821.7	533.1	17,190.45
N1s *	-	-	-	400.0	354.3

* *generically assigned to amino groups.*

The curve-fitted C_{1s} regions are those that are best representing the spectra modifications due to the surface treatments and, here, were fitted this curve using five peaks for the C and six peaks for the CTH.

Peak 1. This is at the lowest BE. This peak could be assigned to extractive compounds [54]. This energy zone is reported for carbides, graphitic compounds, polycyclic carbons, etc. [55].

Peak 2. Contains aromatic carbon (carbon that is bonded to other carbons and/or hydrogen) that is set at 284.8 eV as the internal standard to determine the sample surface charging, and thus, correct the XPS energy scale.

Peak 3. Contains α-carbons, eventual amino and ether groups.

Peak 4. Contains carbon that is singly bonded to oxygen (C-O).

Peak 5. Contains carbonyl-type/carbon that is doubly bonded to oxygen (C = O/O-C-O).

Peak 6. Contains arboxyl-type or similar carbons that are doubly and singly bonded to oxygen.

The region O_{1s} could be curve-fitted with two peaks for both specimens:

1. A peak that was assigned to oxygen that was doubly bonded to carbon.
2. A peak that was assigned to oxygen that was singly bonded to carbon.

The two peaks, which were not clearly resolved in the suitable intensity ratios, using the same full with half-maximum (FWHM), were considered together to be the total O_{1s} area to verify the mass balance with the oxygen-containing carbons which contribute to it, stoichiometrically.

Then the O_{1s} and C_{1s} total areas were derived by summing the normalised areas of all of the peaks that were resolved by curve-fitting, which are listed in Table 4, and these were used to derive the O/C atomic ratio.

If the reported values of the O/C ratio are considered, it can be highlighted that high values signify a high content of cellulose and hemicelluloses, while low values reflect that there is more lignin on the wood surface [56]. In general, this ratio decreased after the thermal modification, due to the dehydration of the cellulose and hemicellulose that was initially present on the wood surface and to the loss of the volatile compounds [53,56]. In contrast, for the deodar cedar wood samples, the O/C ratios, after the thermal modification, increased (from 0.35 to 0.47), which was also observed in the case of jack pine (*Pinus*

banksiana) wood samples [54]. The high content of carbon for unmodified wood surfaces could be an indication of a great number of extractives. The thermal modification removes the extractive compounds [17], thereby increasing the O/C ratio.

Figure 11 compares the labelled wide spectra of the C and CTH samples that were both covered with 5% AKD. The samples that were covered with AKD that was dissolved in toluene at 5% were supposed to cover the wood sample surface with a hydrophobic layer of about 10 nm, i.e., of intermediate thickness, compared to those that are produced by 0.1% and 10% solutions, as reported for thin films of AKD that are grown by spin coating on different substrates from toluene solutions [57].

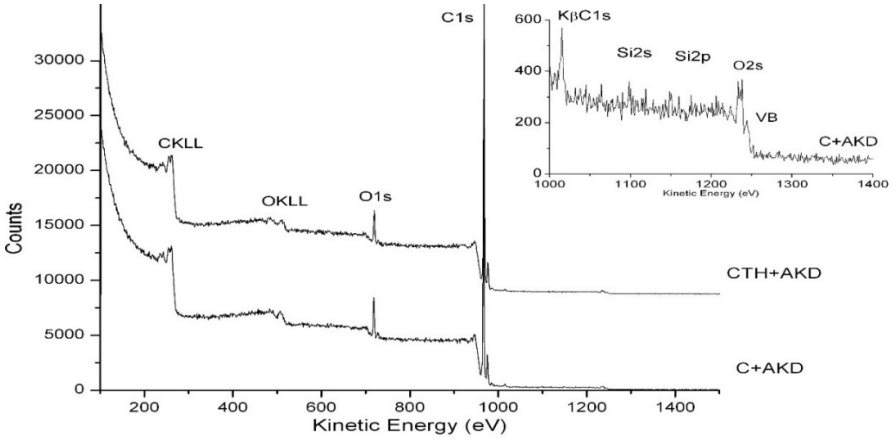

Figure 11. Wide spectrum of thermally modified (CTH + AKD, **top**) and unmodified (C + AKD, **bottom**) cedar wood samples.

The wide spectra of the C and CTH samples that were covered with AKD showed significant differences in comparison to those that are reported in Figure 9 of the same specimens without AKD. In this case, the two wide spectra are similar to each other and, importantly, they both show the carbon and oxygen 1s peak shape and their relative intensity which are similar to those that were reported by Shen et al. [58] for the AKD C18 compound.

Figure 12 compares the curve-fitted C1s regions of the C and CTH samples that were covered with 5% AKD, and Table 5 shows the relevant parameters of the detailed regions that were resolved by the curve-fitting.

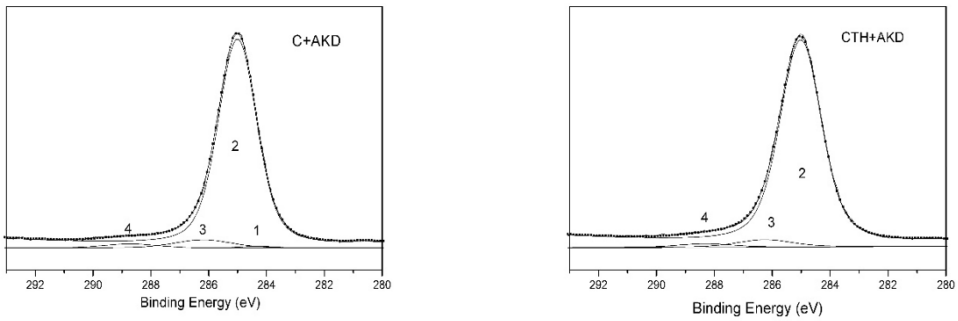

Figure 12. C_{1s} curve-fitted regions of thermally modified (CTH + AKD) and unmodified (C + AKD) cedar wood samples.

Table 5. Fitting parameters of the detailed regions related to the 5% AKD-covered C and CTH samples.

Region	Peak Number	C + 5% AKD		CTH + 5% AKD	
		BE (Ev)	Norm. Area (a.u.)	BE (Ev)	Norm. Area (a.u.)
1_S	1	284.3	498.5.0	-	-
	2	285.0	50614.4	285.0	52104.0
	3	286.2	2954.9	286.2	2477.4
	4	288.7	1477.4	288.3	1238.7
O_{1s}	1	532.4	1430.5	532.3	1321.7
	2	533.4	1430.5	533.5	1321.7
Si_{2p}	-	102.0	162.1	-	-

The regions of C_{1s} were fitted with four and three peaks for the C + 5% AKD and CTH + 5% AKD samples, respectively, and so, they were assigned to:

Peak 1. This was visible at the lowest BE, only for the C + 5% AKD sample, and this could be associated with the presence of silicon and Si2p at 102.0 eV which is assignable to >Si-O that is bonded to carbons [NIST database].

Peak 2. Contains aliphatic carbon (carbon that is bonded to other carbons and/or hydrogen) that is set at 285.0 eV and is used as an internal standard for the BEs correction.

Peak 3. Contains carbon that is singly bonded to oxygen (C-O), plus carbon in alpha to C=O in the lactone ring.

Peak 4. Contains carbonyl carbon in the lactone ring.

The O1s regions were again fitted using two peaks:

1. A peak that is assigned to oxygen that is doubly bonded to carbon.
2. A peak that is assigned to oxygen that is singly bonded to carbon.

In this case, the detailed C_{1s} and O_{1s} regions were fitted by considering the generic AKD formula, which was reported above, and by trying to resolve the two oxygen peaks to properly balance the two carbon-containing oxygen of the lactone ring i.e., the peak n. 3 was made of two carbons that were superimposing in energy (marked with an asterisk in Figure 13) and it was required to be double that of the area of peak n. 4 (lactone carbonyl) and of the corresponding O_{1s} peak 1. Also, the O_{1s} peaks 1 and 2 were required to be in the same area of the carbonyl carbon. The assignments were attempted by referring to the XPS handbook for organic polymers [55].

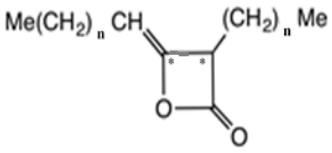

Figure 13. Molecular structure of Alkyl ketene dimers (AKDs).

A satisfying mass balance, which was within the limit of XPS accuracy (±10%), was achieved for both of the wood samples (C and CTH) that were covered with AKD, as can be derived by the normalised areas that are reported in Table 5 by allowing the software *NewGoogly* to adjust the FWHM of each of the component peaks of both the C1s and O1s regions. The total C/O ratio that was obtained for both of the specimens (20.4 and 21.1 for C + AKD and CTH + AKD, respectively) was slightly higher than the value that was corresponding to the stoichiometric ratio of the C18 AKD molecule, as reported by Shen et al. [58]. This could be explained by the greater intensity of the alkyl chains that are exposed outwards, and are depicted along the surface that was analysed by the XPS. A

homogeneous AKD coating was added to the samples with a thickness that was greater than 10 nm (the XPS sampling depth reachable with Mg/Al Kα sources), thus masking both of the sample surfaces, C and CTH, which were chemically different, and their interface bonds eventually formed with the AKD [59].

4. Conclusions

This study investigated the combined effect of thermal modification and the application of AKD on the physical and chemical properties of a deodar cedar wood surface. The results indicated that all of the physicochemical characteristics of this solid material were significantly changed after both of the modifications. Markedly, the results after the irradiation test indicated, also, that thermally modifying the wood had no permanent effect. The influence of the thermal modification on hydrophobicity was negligible, compared to the significant effect of the AKD application. The AKD application at 5% *w*/*w* could be considered as an alternative compound that is useful to make waterproof cedar wood surfaces. XPS is sensitive to surface modifications, and it clearly highlighted the compositional differences of the cedar wood surfaces before (C) and after the thermal modification (CTH). It also confirmed that the surface coverage with 5% AKD is at least 10 nm thick (i.e., above the sampling depth of the technique) and laterally, over the analysed areas, it is homogeneously distributed, thus supporting the WCA measurements and the microscopic views of similar AKD coatings that have been reported in the literature for different substrates.

The FTIR spectra before the weathering test showed that the hydrophobicity was in the absorption band that was between 1700 cm^{-1} and 1750 cm^{-1}, which is related to the formation of the carbonyl groups originating from the reaction between the AKD and hydroxyl groups of cellulose. During the irradiation test, the degradation of the amorphous cellulose component was more intense. In contrast to that which was claimed by other research groups, the absorbance to stretching vibration of acetyl or carboxylic acid at 1730 cm^{-1} decreased significantly, showing that the photoisomerisation to the enolic form occurred. After the thermal modification, the colour of the cedar wood surface changed rapidly from light to dark, i.e., a photo-discolouration and photodegradation processes occurred. The UV light induced a reduction of the protection, also, in the case of AKD. The hydrophobicity of the thermo-modified wood was further increased by the AKD pretreatment on the wood surface. After being exposed to radiation, the cedar wood demonstrated, despite the discolouration, great hydrophobicity, which could increase the range of the uses for priceless wood and save maintenance expenses.

Author Contributions: Conceptualisation, T.L. and L.T.; methodology, M.D., A.M.S., W.G.-A., V.L.G. and F.L.; resources, L.T.; writing—original draft preparation, T.L. and L.T.; funding acquisition, L.T. All authors have read and agreed to the published version of the manuscript.

Funding: This research received no external funding.

Data Availability Statement: Not applicable.

Conflicts of Interest: The authors declare no conflict of interest.

References

1. Chen, C.J.; Kuang, Y.D.; Zhu, S.Z.; Burgert, I.; Keplinger, T.; Gong, A.; Li, T.; Berglund, L.; Eichhorn, S.J.; Hu, L.B. Structure-property-function relationships of natural and engineered wood. *Nat. Rev. Mater.* **2020**, *5*, 642–666.
2. Krišťáková, S.; Neykov, N.; Antov, P.; Sedliačiková, M.; Reh, R.; Halalisan, A.F.; Hajdúchová, I. Efficiency of wood-processing enterprises. Evaluation based on DEA and MPI: A comparison between Slovakia and Bulgaria for the period 2014–2018. *Forests* **2021**, *12*, 1026.
3. Feist, W.C. Outdoor wood weathering and protection. Archaeological wood, properties, chemistry, and preservation. *Adv. Chem. Ser.* **1990**, *225*, 263–298.
4. Giordano, G. *Tecnologia Del Legno 1981*; UTET: Torino, Italy, 1981; Volume 1, pp. 938–939.
5. Scheffer, T.C.; Morrell, J.J. *Natural Durability of Wood: A Worldwide Checklist of Species*; Oregon State University edition; College of Forestry, Forest Research Laboratory: Corvallis, OR, USA, 1998. (in English)

6. Sandak, J.; Goli, G.; Cetera, P.; Sandak, A.; Cavalli, A.; Todaro, L. Machinability of minor wooden species before and after modification with thermo-vacuum technology. *Materials* **2017**, *10*, 121. https://doi.org/10.3390/ma10020121.
7. Lovaglio, T.; D'Auria, M.; Rita, A.; Todaro, L. Compositions of compounds extracted from thermo-treated wood using solvents of different polarities. *IForest* **2017**, *10*, 824. https://doi.org/10.3832/ifor2360-010.
8. Nabil, E.; Mahmoud, N.; Youssef, A.; Saber, E.; Kamel, S. Evaluation of physical, mechanical and chemical properties of Cedar and Sycamore woods after heat treatment. *Egypt. J. Chem.* **2018**, *61*, 1131–1149. https://doi10.21608/ejchem.2018.4301.1383.
9. Bal, B.C. Effects of heat treatment on the physical properties of heartwood and sapwood of Cedruslibani. *Bioresources* **2013**, *8*, 211–219.
10. Barkai, H.; Sadiki, M.; El Abed, S.; Moustakhim, M.; Houssaini, M.I.; Koraichi, S.I. Comparison of the evolution of physicochemical properties due to the single and combined adhesion of two species of the Penicillium genus on cedar wood. *J. Mater. Environ. Sci.* **2015**, *6*, 749–755.
11. Ibnsouda, S.K.; Barkai, H.; Elabed, S.; Sadiki, M.; d Boutahari, S.; Mounyr, B. The Effect of Cellulase Treatment Time on the Cedar Wood Surface Physicochemical Properties.*Am. J. Adv. Sci. Res.* **2016**, *3*, 296–304
12. Hakkou, M.; Pétrissans, M.; Gérardin, P.; Zoulalian, A. Investigations of the reasons for fungal durability of heat-treated beech wood. *Polym. Degrad. Stabilty* **2006**, *91*, 393–397. https://doi.org/10.1016/j.polymdegradstab.2005.04.042.
13. Taylor, A.M.; Gartner, B.L.; Morrell, J.J. Heartwood formation and natural durability-a review. *Wood Fiber. Sci.* 2002, 34:587–611.
14. Kirker, G.T.; Blodgett, A.B.; Arango, R.A.; Lebow, P.K.; Clausen, C.A. The role of extractives in naturally durable wood species. *Int. Biodeterior. Biodegrad.* **2013**, *82*, 53–58. https://doi.org/10.1016/j.ibiod.2013.03.007.
15. Papp, E.A.; Csiha, C.; Makk, A.N.; Hofmann, T.; Csoka, L. Wettability of wood surface layer examined from chemical change perspective. *Coatings* **2020**, *10*, 257.
16. Kamperidou, V.; Barboutis, I.; Vasileiou, V. Influence of thermal treatment on mechanical strength of scots pine (*Pinus sylvestris* L.) wood. *Wood Res.* **2014**, *59*, 373-378.
17. Esteves, B.; Pereira, H. Wood modification by heat treatment: A review. *BioResources* **2009**, *4*, 370–404.
18. Hingston, J.A.; Collins, C.D.; Murphy, R.J.; Lester, J.N. Leaching of chromated copper arsenate wood preservatives: A review. *Environ. Pollut.* **2001**, *111*, 53–66. https://doi.org/10.1016/S0269-7491(00)00030-0.
19. Hubbe, M.A. Paper's resistance to wetting–A review of internal sizing chemicals and their effects. *BioResources* **2007**, *2*, 106–145.
20. Yan, Y.; Amer, H.; Rosenau, T.; Zollfrank, C.; Dörrstein, J.; Jobst, C.; Zimmermann, T.; Keckes, J.; Veigel, S.; Gindl-Altmutter, W.; Li, J. Dry, hydrophobic microfibrillated cellulose powder obtained in a simple procedure using alkyl ketene dimer. *Cellulose* **2016**, *23*, 1189–1197.
21. Arminger, B.; Gindl-Altmutter, W.; Keckes, J.; Hansmann, C. Facile preparation of superhydrophobic wood surfaces via spraying of aqueous alkyl ketene dimer dispersions. *RSC Adv.* **2019**, *9*, 24357–24367. https://doi:10.1039/C9RA03700D.
22. Lovaglio, T.; Gindl-Altmutter, W.; Meints, T.; Moretti, N.; Todaro, L. Wetting behaviour of alder (Alnus cordata (Loisel) Duby) wood surface: Effect of thermo-treatment and Alkyl Ketene Dimer (AKD). *Forests* **2019**, *10*, 770. https://doi.org/10.3390/f10090770.
23. Pouzet, M.; Gautier, D.; Charlet, K.; Dubois, M.; Beakou, A. How to decrease the hydrophilicity of wood flour to process efficient composite materials. *Appl. Surf. Sci.* **2015**, *353*, 1234–1241.
24. Hui, B.; Li, Y.; Huang, Q.; Li, G.; Li, J.; Cai, L.; Yu, H. Fabrication of smart coatings based on wood substrates with photoresponsive behavior and hydrophobic performance. *Mater. Des.* **2015**, *84*, 277–284.
25. Ferrari, S.; Cuccui, I..; Allegretti, O. Thermo-vacuum modification of some European softwood and hardwood species treated at different conditions. *BioResources* **2013**, *8*, 1100–1109.
26. *CSN EN 927-6*; Paints and varnishes—Coating materials and coating systems for exterior wood—Part 6: Exposure of wood coatings to artificial weathering using fluorescent UV lamps and water. European Committee for Standardization: Brussels, Belgium, 2006.
27. de Meijer, M.; Haemers, S.; Cobben, W.; Militz, H. Surface energy determinations of wood: Comparison of methods and wood species. *Langmuir* **2000**, *16*, 9352–9359. https://doi.org/10.1021/la001080n.
28. Meints, T.; Teischinger, A.; Stingl, R.; Hansmann, C. Wood colour of central European wood species: CIELAB characterisation and colour intensification. *Eur. J. Wood Wood Prod*. **2017**, *75*, 499–509.
29. Watts, J.F. *An Introduction to Surface Analysis by Electron Spectroscopy*; (Royal Microscopical Society Microscopy Handbooks, 22); Oxford University Press: New York, NY, USA, 1990; Volume 22, pp. 96.
30. Briggs, D. Practical surface analysis. *Auger X-Ray PhotoelectonSpectroscopy* **1990**, *1*, 151–152.
31. Matthew, J. *Surface Analysis by Auger and X-ray Photoelectron Spectroscopy*; Briggs, D., Grant, J.T., Eds.; IMPublications: Chichester, UK; SurfaceSpectra: Manchester, UK, 2004; p. 900.
32. Castle, J.E.; Salvi, A.M. Chemical state information from the near-peak region of the X-ray photoelectron background. *J. Electron Spectrosc.* **2001**, *114*, 1103–1113. https://doi.org/10.1016/S0368-2048(00)00305-4.
33. Castle, J.E.; Chapman-Kpodo, H.; Proctor, A.; Salvi, A.M. Curve-fitting in XPS using extrinsic and intrinsic background structure. *J. Electron Spectrosc.* **2000**, *106*, 65–80. https://doi.org/10.1016/S0368-2048(99)00089-4.
34. Vogler, E.A. Structure and reactivity of water at biomaterial surfaces. *Adv. Colloid. Interfac.* **1998**, *74*, 69–117. https://doi.org/10.1016/S0001-8686(97)00040-7.
35. Podgorski, L.; Chevet, B.; Onic, L.; Merlin, A. Modification of wood wettability by plasma and corona treatments. *Int. J. Adhes. Adhes.* **2000**, *20*, 103–111. https://doi.org/10.1016/S0143-7496(99)00043-3.

36. Fengel, D.; Wegener, G. Wood: Chemistry, ultrastructure, reactions. *Walter Gruyter* **1984**, *613*, 1960–1982.
37. Tjeerdsma, B.F.; Militz, H. Chemical changes in hydrothermal treated wood: FTIR analysis of combined hydrothermal and dry heat-treated wood. *Holz Roh Werkst.* **2005**, *63*, 102–111. https://doi.org/10.1007/s00107-004-0532-8.
38. Hillis, W.E. High temperature and chemical effects on wood stability. *Wood. Sci. Technol.* **1984**, *18*, 281–293. https://doi.org/10.1007/BF00353364.
39. Shi, Z.; Fu, F.; Wang, S.; He, S.; Yang, R. Modification of Chinese fir with al-kyl ketene dimer (AKD): Processing and characterization. *BioResources* **2013**, *8*, 581–591.
40. Kocaefe, D.; Poncsak, S.; Doré, G.; Younsi, R. Effect of heat treatment on the wettability of white ash and soft maple by water. *Holz Roh Werkst.* **2008**, *66*, 355–361. https://doi.org/10.1007/s00107-008-0233-9.
41. Rowell, R.M. (Ed.) Chemical Modification of Wood. In *Handbook of Wood Chemistry and Wood Composites*, 1st ed.; CRC Press: Boca Raton, FL, USA, 2005; pp. 381. https://doi.org/10.1201/9780203492437.
42. Evans, P.A. Differentiating "hard" from "soft" woods using Fourier transform infrared and Fourier transform spectroscopy. *Spectrochim. Acta Part A Mol. Spectrosc.* **1991**, *47*, 1441–1447. https://doi.org/10.1016/0584-8539(91)80235-B.
43. Colom, X.; Carrillo, F.; Nogués, F.; Garriga, P. Structural analysis of photodegraded wood by means of FTIR spectroscopy. *Polym. Degrad. Stabilty* **2003**, *80*, 543–549. https://doi.org/10.1016/S0141-3910(03)00051-X.
44. Hon, N.S. (1989). *Surface Chemistry of Oxidized Wood. Cellulose and Wood Chemistry and Technology*; Schuerch, C., Ed.; John Wiley and Sons: New York, NY, USA, 1989; p. 1401.
45. Markov, P.; Shishkova, L.; Radushev, A. Effect of UV irradiation on some β-dicarbonyl compounds in solution. *Tetrahedron* **1973**, *29*, 3203–3205. https://doi.org/10.1016/S0040-4020(01)93467-2.
46. Veierov, D.; Bercovici, T.; Fischer, E.; Mazur, Y.; Yogev, A. Photoisomerization of the enol form of 1, 3-dicarbonyl compounds. *J. Am. Chem. Soc.* **1977**, *99*, 2723–2729. https://doi.org/10.1021/ja00450a053.
47. Lozada-Garcia, R.R.; Ceponkus, J.; Chin, W.; Chevalier, M.; Crépin, C. Acetylacetone in hydrogen solids: IR signatures of the enol and keto tautomers and UV induced tautomerization. *Chem. Phys. Lett.* **2011**, *504*, 142–147. https://doi.org/10.1016/j.cplett.2006.09.037.
48. Mitsui, K.; Takada, H.; Sugiyama, M.; Hasegawa, R. Changes in the Properties of Light-Irradiated Wood with Heat Treatment. *Part 1 Eff. Treat. Cond. Change Color* **2001**, *55*, 601–605. https://doi.org/10.1007/s00107-003-0436-z.
49. Bekhta, P.; Niemz, P. Effect of High Temperature on the Change in Color, Dimensional Stability and Mechanical Properties of Spruce Wood. *Holzforschung* **2003**, *57*, 539–546. https://doi.org/10.1515/HF.2003.080.
50. Lebo, S.E.; Lonsky, W.F.; McDonough, T.J.; Medvecz, P.J.; Dimmel, D.R. The occurrence and light-induced formation of ortho-quinonoid lignin structures in white spruce refiner mechanical pulp. *J. Pulp Paper Sci.* **1990**, *16*, 139–143.
51. Pandey, K.K. Study of the effect of photo-irradiation on the surface chemistry of wood. *Polym. Degrad. Stabilty* **2005**, *90*, 9–20. https://doi.org/10.1016/j.polymdegradstab.2005.02.009.
52. Miklecic, J.; Jirouš-Rajković, V.; Antonović, A.; Španić, N. Discolouration of thermally modified wood during simulated indoor sunlight exposure. *BioResources* **2011**, *6*, 434–446.
53. Todaro, L.; D'Auria, M.; Langerame, F.; Salvi, A.M.; Scopa, A. Surface characterization of untreated and hydro-thermally pretreated Turkey oak woods after UV-C irradiation. *Surf. Interface Anal.* **2015**, *47*, 206–215. https://doi.org/10.1002/sia.5689.
54. Kamdem, D.P.; Riedl, B.; Adnot, A.; Kaliaguine, S. ESCA spectroscopy of poly (methyl methacrylate) grafted onto wood fibers. *J. Appl. Polym. Sci.* **1991**, *43*, 1901–1912. https://doi.org/10.1002/app.1991.070431015.
55. Hantsche, H. *High Resolution XPS of Organic Polymers, the Scienta ESCA300 Database*; Beamson, G., Briggs, D., Eds.; Wiley: Chichester, UK, 1992; p. 295, ISBN 0-471-93592-1.
56. Kocaefe, D.; Huang, X.; Kocaefe, Y.; Boluk, Y. Quantitative characterization of chemical degradation of heat-treated wood surfaces during artificial weathering using XPS. *Surf. Interface Anal.* **2013**, *45*, 639–649. https://doi.org/10.1002/sia.5104.
57. Lindfors, J. *Adhesion of Reactive Sizes and Paper Machine Fouling*; University of Technology: Helsinki, Finland, 2007; p. 61.
58. Shen, W.; Zhang, H.; Ettl, R. Chemical composition of "AKD vapour" and its implication to AKD vapour sizing. *Cellulose* **2005**, *12*, 641–652. https://doi.org/10.1007/s10570-005-9010-7.
59. Lindfors, J.; Salmi, J.; Laine, J.; Stenius, P. AKD and ASA model surfaces: Preparation and characterization. *BioResources* **2007**, *2*, 652–670.